The $Z \rightarrow b\bar{b}$ Excess and Top Decay

Ernest Ma

Department of Physics, University of California, Riverside, CA 92521

Daniel Ng

TRIUMF, 4004 Wesbrook Mall, Vancouver, B.C., V6T 2A3, Canada

Abstract

The apparent excess of $Z \rightarrow b\bar{b}$ events at LEP may be an indication of new physics beyond the standard model. However, in either the two-Higgs-doublet model or the minimal supersymmetric standard model, any explanation would lead to an important new decay mode of the top quark and suppresses the $t \rightarrow Wb$ branching fraction, which goes against what has been observed at the Tevatron. In the two-Higgs-doublet model, the branching fraction of $Z \rightarrow b\bar{b}$ + a light boson which decays predominantly into $b\bar{b}$ would be at least of order 10^{-4}.

I. INTRODUCTION

With an accumulation of 8×10^6 Z decays into hadrons and charged leptons by the four LEP experiments at CERN by the end of 1993, measurements of a large number of rates, branching fractions, and asymmetries have now become even more precise [1]. The only apparent deviation by two or more standard deviations from the prediction of the standard model is in the ratio

$$R_b \equiv \frac{\Gamma(Z \to b\bar{b})}{\Gamma(Z \to \text{hadrons})}. \tag{1}$$

Assuming $m_t = 175 \, \text{GeV}$ and $m_H = 300 \, \text{GeV}$, the standard model predicts that $R_b = 0.2158$, whereas LEP obtained $R_b = 0.2202 \pm 0.0020$ if the similarly defined R_c is assumed to be independent. If the latter is fixed at its standard-model value, then $R_b = 0.2192 \pm 0.0018$. In either case, the excess is about $2\% \pm 1\%$. If this is taken seriously, physics beyond the standard model is indicated.

In this paper we will examine two frequently studied extensions of the standard model: the two-Higgs-doublet model (2HDM) and the minimal supersymmetric standard model (MSSM). We will assume that the only significant deviation from the standard model is R_b, hence we will take $R_b = 0.2192 \pm 0.0018$ as the experimental value and see how these two extensions may be able to explain it. We will concentrate on obtaining $R_b > 0.2174$, *i.e.* within one standard deviation of the experimental value, because otherwise the difference with the standard model is insignificant and we might as well not bother with any possible extension.

Whereas the contributions to R_b from either the 2HDM [2–5] or the MSSM [6–8] have been studied previously, we are concerned here also with the effect of these new contributions on top decay. Together with the constraints from the oblique parameters [9], we find that a large R_b excess will always lead to an important new decay mode of the top quark and suppresses the $t \to Wb$ branching fraction, which goes against what has been observed at the Fermilab Tevatron [10]. In the 2HDM, we also find that the branching fraction of $Z \to b\bar{b}$ + a light boson which decays predominantly into $b\bar{b}$ will be at least of order 10^{-4} [11].

II. TWO HIGGS DOUBLETS

The simplest extension of the standard model is to have two Higgs doublets instead of just one. The relevance of this model to R_b was studied in detail already a few years ago [2]. To establish notation, let the two Higgs doublets be given by

$$\Phi_i = \begin{pmatrix} \phi_i^+ \\ \phi_i^0 \end{pmatrix} = \begin{pmatrix} \phi_i^+ \\ (v_i + \eta_i + i\chi_i)/\sqrt{2} \end{pmatrix} . \tag{2}$$

Let $\tan\beta \equiv v_2/v_1$, then

$$h^+ = \phi_2^+ \cos\beta - \phi_1^+ \sin\beta , \tag{3}$$

$$A = \chi_2 \cos\beta - \chi_1 \sin\beta , \tag{4}$$

$$h_1 = \eta_1 \cos\alpha + \eta_2 \sin\alpha , \tag{5}$$

$$h_2 = \eta_2 \cos\alpha - \eta_1 \sin\alpha . \tag{6}$$

The corrections to the left- and right-handed $Zb\bar{b}$ vertex induced by the charged Higgs boson h^+ and the neutral Higgs bosons h_1, h_2 and A are given by [2]

$$\delta g_{L,R}^b(h^+) = \frac{\alpha}{4\pi s_W^2} \lambda_{L,R}^2 \, \rho_{L,R}^C(q^2, m_+^2, m_t^2) , \tag{7}$$

and

$$\delta g_{L,R}^b(h_{1,2}, A) = \frac{\alpha}{4\pi s_W^2} \left(\frac{m_b \tan\beta}{2m_W}\right)^2 [\cos^2\alpha \, \rho_{L,R}^N(q^2, m_1^2, m_A^2) + \sin^2\alpha \, \rho_{L,R}^N(q^2, m_2^2, m_A^2)] , \tag{8}$$

where

$$\rho_{L,R}^C(q^2, m^2, M^2) = \{-,+\}\tfrac{1}{2}m_t^2 C_0(q^2, m^2, M^2, M^2) + g_{L,R}^b \, \rho_3(q^2, m^2, M^2, M^2)$$
$$+ g^h \left[\rho_3(q^2, m^2, M^2, M^2) - \rho_4(q^2, m^2, m^2, M^2)\right] , \tag{9}$$

$$\rho_{L,R}^N(q^2, m^2, M^2) = \{-,+\}\rho_4(q^2, m^2, M^2, 0) + g_{R,L}^b \left[\rho_3(q^2, m^2, 0, 0) + \rho_3(q^2, M^2, 0, 0)\right] . \tag{10}$$

In the above, $g_L^b = -\frac{1}{2} + \frac{1}{3}s_W^2$, $g_R^b = \frac{1}{3}s_W^2$ and $g^h = \frac{1}{2} - s_W^2$. We have also assumed that Φ_2 couples to the up-type quarks and Φ_1 to the down-type quarks, hence $\lambda_L = \frac{m_t}{\sqrt{2}m_W} \cot\beta$,

3

and $\lambda_R = \frac{m_b}{\sqrt{2}m_W}\tan\beta$. The masses of h^+, h_1, h_2 and A are denoted by m_+, m_1, m_2, and m_A respectively. The functions C_0 and $\rho_{3,4}$ are defined in Ref. [2]; see also Appendix A.

For a heavy top quark, it is well-known that $\rho_{L,R}^C(q^2, m_+^2, m_t^2) \simeq \{-,+\}(-\frac{1}{2})$. Hence $g_L^b \mathrm{Re}\{\delta g_L^b(h^+)\}$ and $g_R^b \mathrm{Re}\{\delta g_R^b(h^+)\}$ are negative, thereby decreasing the value of R_b. This means that the $\tan\beta < 1$ region can be ruled out [3–5]. In this region, $t \to bh^+$ also becomes the dominant decay for the top quark [12] unless it is kinematically not allowed. In fact, any significant reduction of the $t \to Wb$ branching fraction is in conflict with the Tevatron data [10] because the number of top events observed is such that even if we assume $B(t \to Wb) = 1$, the deduced experimental $t\bar{t}$ production cross section is already larger than expected [13].

If $\tan\beta$ is large, the contribution from the neutral Higgs bosons becomes important. In other words, Eq. (8) must be considered even though it is suppressed by $(m_b/m_W)^2$. Note that since R_b is proportional to $(g_L^b + \delta g_L^b)^2 + (g_R^b + \delta g_R^b)^2$, ρ_L^N is more important than ρ_R^N because $g_L^b >> g_R^b$ [3]. Again because g_R is small, ρ_L^N is dominated by $\rho_4(q^2, m^2, M^2, 0)$ in Eq. (10). In order that $\rho_4(q^2, m^2, M^2, 0)$ be positive and not too small, both m and M must be light, namely $m^2, M^2 < q^2$. In particular, for $\rho_4(m_Z^2, m^2, M^2, 0) \geq 0.2$, both m and M should be less than 65 GeV.

It was shown already in Ref. [2] that for $\tan\beta = 70 \simeq 2m_t/m_b$, the R_b excess peaks at about 4% near $m_A = m_1 \simeq 40$ GeV for $\alpha = 0$. However, since $Z \to Ah_1$ is not observed, $m_A + m_1 > m_Z$ is a necessary constraint. We show in Fig. 1 the contours in the $m_1 - m_A$ plane for $R_b = 0.2192$ and 0.2174. It is clear that relatively light scalar bosons are required if the R_b excess is to be explained.

For $A(h_1)$ lighter than m_Z and having an enhanced coupling to $b\bar{b}$, the decay $Z \to b\bar{b} + A(h_1)$ becomes nonnegligible [14]. As an illustration, we show in Fig. 2 the branching fractions of these two decays as functions of m_A with the constraint $m_A + m_1 = m_Z + 10$ GeV so that a reasonable fit to the R_b excess is obtained. It is seen that the sum of these two branching fractions is at least of order 10^{-4}. Once produced, A or h_1 decays predominantly into $b\bar{b}$ as well. Hence this scenario for explaining R_b can be tested at LEP if the sensitivity

for identifying one $b\bar{b}$ pair as coming from A or h_1 in $b\bar{b}b\bar{b}$ final states can be pushed down below 10^{-4}.

Since b_L is involved in any enhanced coupling to light particles in explaining the R_b excess, its doublet partner t_L must necessarily have the same enhanced coupling to related particles. In the 2HDM, we must have an enhanced $\bar{t}bh^+$ coupling. Therefore, unless $m_+ > m_t - m_b$, the branching fraction of $t \to bh^+$ will be important. As a result, the standard $t \to Wb$ branching fraction will be seriously degraded. We show this in Fig. 3 as a function of m_+. Large values of m_+ are disfavored in this scenario because the splitting with A and h_1 would result in a large contribution to the oblique parameter T, resulting in the constraint $m_+ \leq 150$ GeV [4].

III. SUPERSYMMETRIC HIGGS SECTOR

In the minimal supersymmetric standard model (MSSM), the two Higgs doublets have exactly the same gauge and Yukawa couplings as in the 2HDM we discussed in the previous section. In addition, the quartic scalar couplings of the MSSM are determined by the gauge couplings and there are only three arbitrary mass terms: $\Phi_1^\dagger \Phi_1$, $\Phi_2^\dagger \Phi_2$, and $\Phi_1^\dagger \Phi_2 + \Phi_2^\dagger \Phi_1$. Hence we need only two extra parameters, usually taken to be $\tan\beta$ and m_A, to specify the entire Higgs sector, subject of course to radiative corrections [15]. However, these corrections are only significant for small $\tan\beta$ and since we need a large $\tan\beta$ to explain R_b, we will use the simpler tree-level expressions in our numerical analysis. Combining both the charged and neutral Higgs contributions, we plot in Fig. 4 the $R_b = 0.2192$ and 0.2174 contours in the $m_A - \tan\beta$ plane, with the constraint $m_A + m_1 > m_Z$. We plot also the contours for $B(t \to Wb) = 0.85$ and 0.7, which correspond to reductions of 28% and 51% of the top signals at Fermilab respectively. It is abundantly clear that the Higgs sector of the MSSM is not compatible with both a large R_b and a small $B(t \to bh^+)$. In the 2HDM, m_A and m_+ are independent parameters, whereas in the MSSM, there is the well-known sum rule $m_+^2 = m_A^2 + m_W^2$. Hence an approximate custodial symmetry exists in the MSSM to keep the

contribution to T small, but at the same time $m_+ < m_t - m_b$ is inevitable if m_A is assumed to be small enough to obtain a large R_b excess. In Fig. 5 we plot the minimum branching fraction $B(Z \to b\bar{b}A + b\bar{b}h_1)$ for a given lower bound of R_b. This minimum is obtained by varying $\tan\beta$ with a fixed value of m_A. As in Fig. 2, we see that this branching fraction is at least of order 10^{-4}.

IV. CHARGINOS AND NEUTRALINOS

In addition to the Higgs contributions, there are chargino (χ) and neutralino ($\mathcal{N}$) contributions to R_b in the MSSM. They have been studied previously [6–8], and it is known that the particles in the loops have to be light in order to obtain large contributions. The parameters involved here are $\tan\beta$, μ, M_2, $m_{\tilde{t}_{1,2}}$, $m_{\tilde{b}_{1,2}}$, $\theta^{\tilde{t}}$, and $\theta^{\tilde{b}}$, where the supergravity condition $M_1 \sim 0.5 M_2$ at the electroweak scale has been assumed. The scalar mixing angles $\theta^{\tilde{t}}$ and $\theta^{\tilde{b}}$ as well as others are defined in Appendix B.

Since scalar quarks have not been observed at LEP, their masses must be greater than half of the center-of-mass energy, namely $m_{\tilde{t}_1, \tilde{b}_1} \geq \frac{1}{2}m_Z$. On the other hand, the lightest neutralino ($\mathcal{N}_1$) is always lighter than the lightest chargino (χ_1), thus the condition $m_{\chi_1} \geq \frac{1}{2}m_Z$ is not enough by itself. Let us define the conservative constraints from the invisible width and total width of Z as $\delta\Gamma_{\rm inv} \equiv \Gamma_{\rm inv}({\rm expt})|_{\rm max} - \Gamma_{\rm inv}({\rm SM})|_{\rm min}$ and $\delta\Gamma_Z \equiv \Gamma_Z({\rm expt})|_{\rm max}$ - $\Gamma_Z({\rm SM})|_{\rm min}$, where SM denotes the standard model.

From the updated LEP data [1], we obtain

$$\Gamma(Z \to \mathcal{N}_1\mathcal{N}_1) \leq \delta\Gamma_{\rm inv} = 7.6 \text{ MeV} , \tag{11}$$

$$\Gamma(Z \to \mathcal{N}_i\mathcal{N}_j) \leq \delta\Gamma_Z = 23 \text{ MeV} . \tag{12}$$

These constraints must be included for the analysis in order to provide consistent results.

The corrections to the left- and right-handed $Zb\bar{b}$ vertex induced by the charginos (χ) and neutralinos ($\mathcal{N}$) are given by

$$\delta g_{L,R}^b(\chi,\mathcal{N}) = \frac{\alpha}{4\pi s_W^2} F_{L,R}(\chi,\mathcal{N}) , \tag{13}$$

where

$$F_{L,R}(\chi) = \Lambda_{jk}^{L,R*} \, S_{ji}^t \, \Lambda_{ik}^{L,R} \, \rho_4(q^2, m_{\tilde{t}_i}^2, m_{\tilde{t}_j}^2, m_{\chi_k}^2) - \Lambda_{ki}^{L,R} \, \mathcal{O}_{ij}^{L,R} \, \Lambda_{kj}^{L,R*} \, \rho_3(q^2, m_{\tilde{t}_k}^2, m_{\chi_i}^2, m_{\chi_j}^2)$$

$$+\Lambda_{ki}^{L,R} \, (\mathcal{O}_{ij}^{R,L} - \mathcal{O}_{ij}^{L,R}) \, \Lambda_{kj}^{L,R*} \, m_{\chi_i} \, m_{\chi_j} \, C_0(q^2, m_{\tilde{t}_k}^2, m_{\chi_i}^2, m_{\chi_j}^2) \,, \qquad (14)$$

$$F_{L,R}(\mathcal{N}) = \lambda_{jk}^{L,R*} \, S_{ji}^b \, \lambda_{ik}^{L,R} \, \rho_4(q^2, m_{\tilde{b}_i}^2, m_{\tilde{b}_j}^2, m_{\mathcal{N}_k}^2) - \lambda_{ki}^{L,R} \, \mathcal{Q}_{ij}^{L,R} \, \lambda_{kj}^{L,R*} \, \rho_3(q^2, m_{\tilde{b}_k}^2, m_{\mathcal{N}_i}^2, m_{\mathcal{N}_j}^2)$$

$$+\lambda_{ki}^{L,R} \, (\mathcal{Q}_{ij}^{R,L} - \mathcal{Q}_{ij}^{L,R}) \, \lambda_{kj}^{L,R*} \, m_{\mathcal{N}_i} \, m_{\mathcal{N}_j} \, C_0(q^2, m_{\tilde{b}_k}^2, m_{\mathcal{N}_i}^2, m_{\mathcal{N}_j}^2) \,, \qquad (15)$$

and there is an implicit sum over all repeated indices. See Appendix B for the definitions of the various quantities in the above.

For $\tan\beta < 20$ or $m_{\tilde{b}_{1,2}} > m_Z$, the chargino contribution is the most important. From Eq.(14), we see that the contribution is the largest when the lighter scalar quark $\tilde{t}_1$ is mostly $\tilde{t}_R$, namely $\theta_{11}^{\tilde{t}} = 0$. We follow the usual strategy [7] of finding the maximally allowed R_b for a given $\tan\beta$ and m_{χ_1}. Here we impose also the LEP constraints given by Eq.(12). In Fig. 6, we plot the maximally allowed R_b as a function of $\tan\beta$ for $m_{\chi_1} = 60$ GeV and $m_{\tilde{t}_1} = \frac{1}{2}m_Z$. We see that $R_b > 0.217$ can be obtained. However, top decay into $\tilde{t}_1$ and a neutralino is now possible and the corresponding branching fraction $B(t \to Wb)$ shows clearly that this solution would conflict with the Tevatron data [10,13].

If $\tan\beta$ is large, the neutralino contributions become important because the b quark coupling to the higgsino is proportional to $1/\cos\beta$. Here we would like to point out that our $\tilde{b}_i \overline{\mathcal{N}_j^C}^* b$ couplings given in Eqs. (B15) and (B16) are different from those given in Ref. [7] but agree with Ref. [16]. For simplicity and with little loss of generality, we assume that $m_{\tilde{t}_1} = m_{\tilde{b}_1} = 60$ GeV and $m_{\tilde{t}_2} = m_{\tilde{b}_2} = 250$ GeV. We vary the scalar quark mixing angles $\theta^{\tilde{t}}$ and $\theta^{\tilde{b}}$, such that R_b is maximum within the allowed LEP constraints given by Eq.(12) and $m_{\chi_1} > \frac{1}{2}m_Z$. This is the most optimistic scenario; we cannot achieve a large enough R_b otherwise. Taking $\tan\beta = 70$, the contours of $R_b = 0.2174$ and 0.2192 are plotted in Fig. 7. Again we plot the $t \to Wb$ branching fraction. We find only very narrow regions where $B(t \to Wb) > 0.7$ and $R_b > 0.2174$. Hence future experiments on top decay will play a decisive role to verify or rule out this scenario [17].

The dominant contribution to the oblique parameter T comes from the scalar quarks.

We have checked that $T \sim 0.4$ in the narrow regions, which is in mild conflict with the recent global fit $T = -0.67 \pm 0.92$ [18]. Nevertheless, Fig. 7 represents the most optimistic scenario. In Fig. 8, we consider a more restrictive case with $\theta^{\tilde{t}} = \theta^{\tilde{b}}$ so that $T = 0$. As a result, the narrow regions shrink as expected.

V. CONCLUSION

The 2HDM [2–5] and the MSSM [6–8] have each been suggested to explain the R_b excess at LEP. Here we consider also the effects of these new contributions on top quark decay. In the 2HDM, large $\tan\beta$ and light neutral scalars are necessary to increase R_b to within one standard deviation of the experimental value. The corresponding $\bar{t}bh^+$ coupling then allows top decay into b and h^+ unless it is kinematically not allowed. However, $m_+ > 150$ GeV would be in conflict with the constraint of the oblique parameter T. The same interactions which allow a large R_b also allow the decays $Z \rightarrow b\bar{b}A(h_1)$. We show in Fig. 2 that the branching fraction $B(Z \rightarrow b\bar{b}A + b\bar{b}h_1)$ is at least of order 10^{-4} which can be tested at future LEP experiments.

In the supersymmetric Higgs sector, there are only two independent unknown parameters: $\tan\beta$ and m_A. Specifically, because of the sum rule $m_+^2 = m_A^2 + m_W^2$, top decay is always possible for a small enough m_A to account for the R_b excess. We see in Fig. 4 that the region which allows R_b to be large does indeed conflict with top decay. In addition, $B(Z \rightarrow b\bar{b}A + b\bar{b}h_1)$ is also at least of order 10^{-4} as shown in Fig. 5.

Because of the scalar-quark mixing angles, the chargino and neutralino contributions to R_b could each be either positive or negative. Here we consider the most optimistic scenario that the mixing angles are chosen to maximize the R_b value. The chargino contribution, as opposed to the charged Higgs and W contributions, can increase R_b above 0.2174 if $\tilde{t}_1$ and χ_1 are light enough. Since $\mathcal{N}_1$ is always lighter than χ_1, we impose also the LEP constraints given by Eq. (12). Again this new contribution gives rise to a new channel for top decay which reduces the $t \rightarrow Wb$ branching fraction significantly. For large $\tan\beta$, we consider both

chargino and neutralino contributions. We find that there are only very narrow regions, as shown in Figs. 7 and 8, in which both large R_b and $B(t \to Wb)$ are compatible. Future experiments on top decay would verify or rule out this scenario.

Note added. After the completion of this paper, additional data from LEP have been reported. [19] For R_c fixed at its standard-model value, the latest experimental value of R_b is 0.2205 ± 0.0016. This means that our assertion that R_b conflicts with top decay in the 2HDM and the MSSM becomes even stronger.

APPENDIX A: DEFINITION OF ρ_3

The general form for ρ_3 is given by

$$\rho_3(q^2, m^2, M_1^2, M_2^2) = [q^2(C_{22} - C_{23}) + 2C_{24} - M_1 M_2 C_0](q^2, m^2, M_1^2, M_2^2)$$

$$+ \frac{1}{2}[B_1(0, M_1^2, m^2) + B_1(0, M_2^2, m^2)] - \frac{1}{2}. \tag{A1}$$

For $M_1 = M_2$, ρ_3 is identical to that defined in Ref. [2]. This generalized definition is useful in the supersymmetric case.

APPENDIX B: MASSES AND MIXING IN THE MSSM

In this appendix, we present the relevant couplings for the chargino and neutralino contributions to the $Zb\bar{b}$ vertex. We allow general scalar top mixing, namely $\tilde{t}_L = \theta_{1i}^{\tilde{t}} \, \tilde{t}_i$ and $\tilde{t}_R = \theta_{2i}^{\tilde{t}} \, \tilde{t}_i$ with a similar definition for the scalar bottom quarks. The $Z\tilde{t}_i^*\tilde{t}_j$ and $Z\tilde{b}_i^*\tilde{b}_j$ vertices are given by $\frac{g}{\cos\theta_W} \, S_{ij}^{t,b}(p_i - p_j)_\mu$, where

$$S_{ij}^t = \frac{1}{2}\theta_{1i}^{\tilde{t}}{}^* \theta_{1j}^{\tilde{t}} - \frac{2}{3}\sin^2\theta_W \delta_{ij} , \tag{B1}$$

$$S_{ij}^b = -\frac{1}{2}\theta_{1i}^{\tilde{b}}{}^* \theta_{1j}^{\tilde{b}} + \frac{1}{3}\sin^2\theta_W \delta_{ij} . \tag{B2}$$

The p's are defined as out-going momenta.

The chargino and neutralino mass matrices are given by

$$\mathcal{M}_\chi = \begin{pmatrix} M_2 & \sqrt{2}m_W \cos\beta \\ \sqrt{2}m_W \sin\beta & \mu \end{pmatrix} , \tag{B3}$$

which links $(i\tilde{W}^-, \tilde{h}_1^-)^T$ to $(i\tilde{W}^+, \tilde{h}_2^+)$, and

$$\mathcal{M}_\mathcal{N} = \begin{pmatrix} M_1 & 0 & -m_Z \sin\theta_W \cos\beta & m_Z \sin\theta_W \sin\beta \\ 0 & M_2 & m_Z \cos\theta_W \cos\beta & -m_Z \cos\theta_W \sin\beta \\ -m_Z \sin\theta_W \cos\beta & m_Z \cos\theta_W \cos\beta & 0 & -\mu \\ m_Z \sin\theta_W \sin\beta & -m_Z \cos\theta_W \sin\beta & -\mu & 0 \end{pmatrix} , \tag{B4}$$

in the $(i\tilde{B}, i\tilde{W}_3, \tilde{h}_1^0, \tilde{h}_2^0)$ basis. The mass eigenstates, χ_i and $\mathcal{N}_i$, are related to these basis states by the following transformations:

$$(i\tilde{W}^+, \tilde{h}_2^+)^T = V_{ij}\chi_j \; ; \quad (i\tilde{W}^-, \tilde{h}_1^-)^T = U_{ij}\chi_j^C \; , \tag{B5}$$

and

$$(i\tilde{B}, i\tilde{W}_3, \tilde{h}_1^0, \tilde{h}_2^0)^T = N_{ij}\mathcal{N}_j \; . \tag{B6}$$

Thus, M_χ and $M_\mathcal{N}$ are diagonalized by

$$V^T \, \mathcal{M}_\chi \, U \; = \; m_{\chi_i}\delta_{ij} \; , \tag{B7}$$

and

$$N^T \, \mathcal{M}_\mathcal{N} \, N \; = \; m_{\mathcal{N}_i}\delta_{ij} \; . \tag{B8}$$

Let us first consider the vertices for loops involving charginos χ. The $Z\overline{\chi_i}\chi_j$ vertex is given by $\frac{g}{\cos\theta_W}\gamma_\mu[\mathcal{O}_{ij}^L \frac{1-\gamma_5}{2} + \mathcal{O}_{ij}^R \frac{1+\gamma_5}{2}]$ with

$$\mathcal{O}_{ij}^L = \cos^2\theta_W \; \delta_{ij} - \tfrac{1}{2}V_{2i}^* \, V_{2j} \; , \tag{B9}$$

$$\mathcal{O}_{ij}^R = \cos^2\theta_W \; \delta_{ij} - \tfrac{1}{2}U_{2i} \, U_{2j}^* \; , \tag{B10}$$

and the $\tilde{t}_i^* \overline{\chi_j^C} b$ vertex is given by $g[\Lambda_{ij}^L \frac{1-\gamma_5}{2} + \Lambda_{ij}^R \frac{1+\gamma_5}{2}]$ with

$$\Lambda_{ij}^L = -V_{1i} \, \theta_{1j}^{\tilde{t}\,*} + \frac{m_t}{\sqrt{2}m_W \sin\beta} \, V_{2i} \, \theta_{2j}^{\tilde{t}\,*} \; , \tag{B11}$$

$$\Lambda_{ij}^R = \frac{m_b}{\sqrt{2}m_W \cos\beta} \, U_{2i}^* \, \theta_{1j}^{\tilde{t}\,*} \; . \tag{B12}$$

For the vertices involving neutralino loops, $Z\overline{\mathcal{N}_i}\mathcal{N}_j$ vertex is given by $\frac{g}{\cos\theta_W}\gamma_\mu[\mathcal{Q}_{ij}^L \frac{1-\gamma_5}{2} + \mathcal{Q}_{ij}^R \frac{1+\gamma_5}{2}]$ with

$$\mathcal{Q}_{ij}^L = \tfrac{1}{2}(N_{3i}^* \, N_{3j} - N_{4i}^* \, N_{4j}) \; , \tag{B13}$$

$$\mathcal{Q}_{ij}^R = \tfrac{1}{2}(N_{4i} \, N_{4j}^* - N_{3i} \, N_{3j}^*) \; , \tag{B14}$$

and the $\tilde{b}_i^* \overline{\mathcal{N}_j^C} b$ vertex is given by $g[\lambda_{ij}^L \frac{1-\gamma_5}{2} + \lambda_{ij}^R \frac{1+\gamma_5}{2}]$ with

11

$$\lambda_{ij}^{L} = -\frac{1}{3\sqrt{2}} \, \tan\theta_W \, N_{1i} \, \theta_{1j}^{\tilde{b}}{}^{*} + \frac{1}{\sqrt{2}} N_{2i} \, \theta_{1j}^{\tilde{b}}{}^{*} - \frac{m_b}{\sqrt{2}m_W \cos\beta} \, N_{3i} \, \theta_{2j}^{\tilde{b}}{}^{*} \,, \qquad \text{(B15)}$$

$$\lambda_{ij}^{R} = -\frac{\sqrt{2}}{3} \, \tan\theta_W \, N_{1i}^{*} \, \theta_{2j}^{\tilde{b}}{}^{*} - \frac{m_b}{\sqrt{2}m_W \cos\beta} \, N_{3i}^{*} \, \theta_{1j}^{\tilde{b}}{}^{*} \,. \qquad \text{(B16)}$$

Note that the relative signs of the m_b terms in Eqs. (B15) and (B16) are in agreement with Ref. [16], but differ from Ref. [7].

REFERENCES

[1] The LEP Collaborations: ALEPH, DELPHI, L3, OPAL, and the LEP Electroweak Working Group, CERN Report No. CERN/PPE/94-187 (25 November 1994).

[2] A. Denner, R. J. Guth, W. Hollik, and J. H. Kuhn, Z. Phys. **C51**, 695 (1991).

[3] J. T. Liu and D. Ng, Phys. Lett. **B342**, 262 (1995).

[4] A. K. Grant, Phys. Rev. D **51**, 207 (1995).

[5] G. T. Park, *Implications of the recent top quark discovery on two Higgs doublet model*, hep-ph/9504369, YUMS-95-9, March 1995.

[6] G. Altarelli, R. Barbieri, and F. Caravaglios, Phys. Lett. **B324**, 357 (1993).

[7] J. D. Wells, C. Kolda, and G. L. Kane, Phys. Lett. **B338**, 219 (1994).

[8] D. Garcia, R. A. Jimenez, and J. Sola, Phys. Lett. **B347**, 321 (1995).

[9] M. E. Peskin and T. Takeuchi, Phys. Rev. Lett. **65**, 964 (1990); Phys. Rev. D **46**, 381 (1992).

[10] F. Abe *et al.* (CDF Collaboration), Phys. Rev. Lett. **74**, 2626 (1995); S. Abachi *et al.* (D0 Collaboration), *ibid.* **74**, 2632 (1995).

[11] E. Ma and D. Ng, UCRHEP-T144, TRI-PP-95-16, in Proc. of the International Symposium on Vector Boson Self-Interactions, UCLA, February 1995, to be published.

[12] J. Erler and P. Langacker, " *Implication of High Precision Experiments and the CDF Top Quark Candidates* ", hep-ph/9411203, UPR-0632T, October 1994.

[13] E. Laenen, J. Smith, and W. van Neerven, Phys. Lett. **B321**, 254 (1994).

[14] A. Djouadi, P. M. Zerwas, and J. Zunft, Phys. Lett. **B259**, 175 (1991).

[15] Y. Okada, M. Yamaguchi and T. Yanagida, Phys. Lett. **B262**, 54 (1991); Prog. Theor.

Phys. **85**, 1 (1991); J. Ellis, G. Ridolfi and F. Zwirner, Phys. Lett. **B257**, 83 (1991); H. E. Haber and R. Hempfling, Phys. Rev. Lett. **66**, 1815 (1991).

[16] J. F. Gunion and H. E. Haber, Nucl. Phys. **B272**, 1 (1984).

[17] The relevance of top decay was mentioned recently by G. L. Kane, R. G. Stuart, and J. D. Wells, *A Global Fit of LEP/SLC Data with Light Superpartners*, hep-ph/9505207, UM-TH-95-16 (April 1995); other recent papers on the MSSM include D. Garcia and J. Sola, hep-ph/9502317, UAB-FT-358 (January 1995); P. H. Chankowski and S. Pokorski, hep-ph/9505304, IFT-95/5 (March 1995); A. Dabelstein, W. Hollik, and W. Mosle, hep-ph/9506251, KA-THEP-5-1995 (March 1995); X. Wang, J. Lopez, and D. Nanopoulos, hep-ph/9506217, CTP-TAMU-25/95 (June 1995).

[18] C. P. Burgess, S. Godfrey, H. Konig, D. London, and I. Maksymyk, Phys. Lett. **B326**, 276 (1994).

[19] P. B. Renton, in Proc. of the 17th International Symposium on Lepton-Photon Interactions, Beijing, China (August 1995), to be published.

FIGURES

FIG. 1. $R_b = 0.2192$ (solid) and 0.2174 (dashed) contours in the $m_1 - m_A$ plane for $\alpha = 0$ and $\tan\beta = 70$. The straight line corresponds to $m_A + m_1 = M_Z$. We have also assumed $m_+ = m_2 = 175$ GeV.

FIG. 2. The branching fractions, $B(Z \to b\bar{b}A)$ (dashed) and $B(Z \to b\bar{b}h_1)$ (dotted) and their sum (solid), as functions of m_A where we take $m_A + m_1 = M_Z + 10$ GeV, $\tan\beta = 70$, $\alpha = 0$, and $m_+ = m_2 = 175$ GeV.

FIG. 3. The branching fraction $B(t \to Wb)$ as a function of m_+ for $\tan\beta = 70$ (solid), 50 (dashed), and 20 (dotted).

FIG. 4. $R_b = 0.2192$ (heavy), 0.2174 (solid) and $B(t \to Wb) = 0.85$ (dashed), 0.7 (dotted) contours in the $m_A - \tan\beta$ plane. We also plot the constraint $m_A + m_1 > m_Z$ (dash-dotted).

FIG. 5. The minimum branching fraction $B(Z \to b\bar{b}A + b\bar{b}h_1)$ for a given lower bound of R_b, where we take $m_A = 45$ GeV (solid) and $m_A = 50$ GeV (dashed).

FIG. 6. The maximally allowed R_b (solid) as a function of $\tan\beta$ for $m_{\chi_1} = 60$ GeV and $m_{\tilde{t}_1} = \frac{1}{2}m_Z$. We also plot the corresponding branching ratio $B(t \to bW)$ (dashed). We have assumed $m_{\tilde{t}_2} = 250$ GeV and $\theta^{\tilde{t}}_{12} = 1$.

FIG. 7. Contours of maximally allowed values $R_b = 0.2174$ (solid) and 0.2192 (dotted) as well as $B(t \to Wb) \geq 0.7$ (dashed) in the $\mu - M_2$ plane where the heavy lines represent the LEP constraints and $m_{\chi_1} > \frac{1}{2}m_Z$. We assume $m_{\tilde{t}_1} = m_{\tilde{b}_1} = 60$ GeV and $m_{\tilde{t}_2} = m_{\tilde{b}_2} = 250$ GeV.

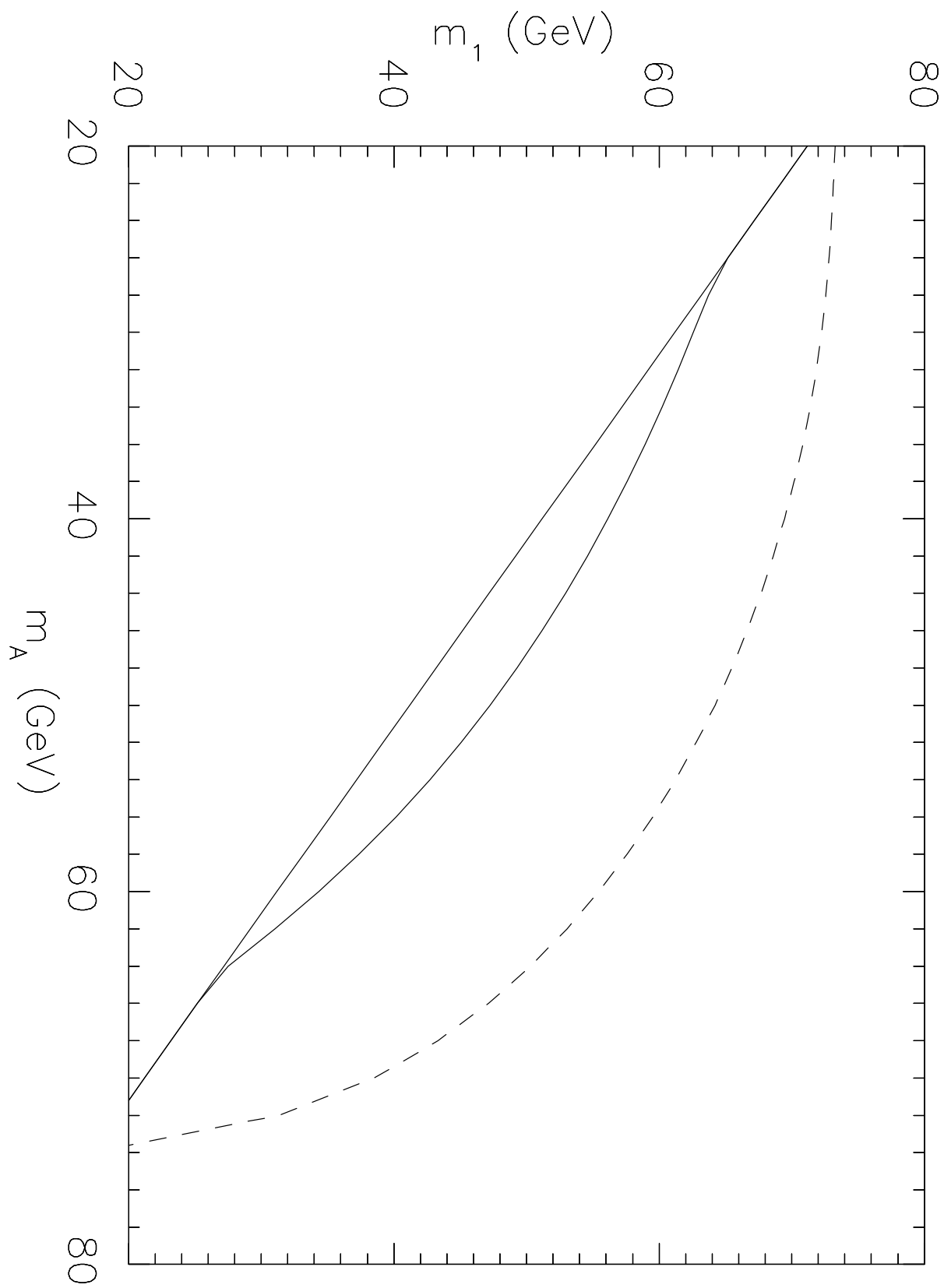FIG. 8. The same as Fig. 7 but with the added constraint $\theta^{\tilde{t}} = \theta^{\tilde{b}}$ so that $T = 0$.
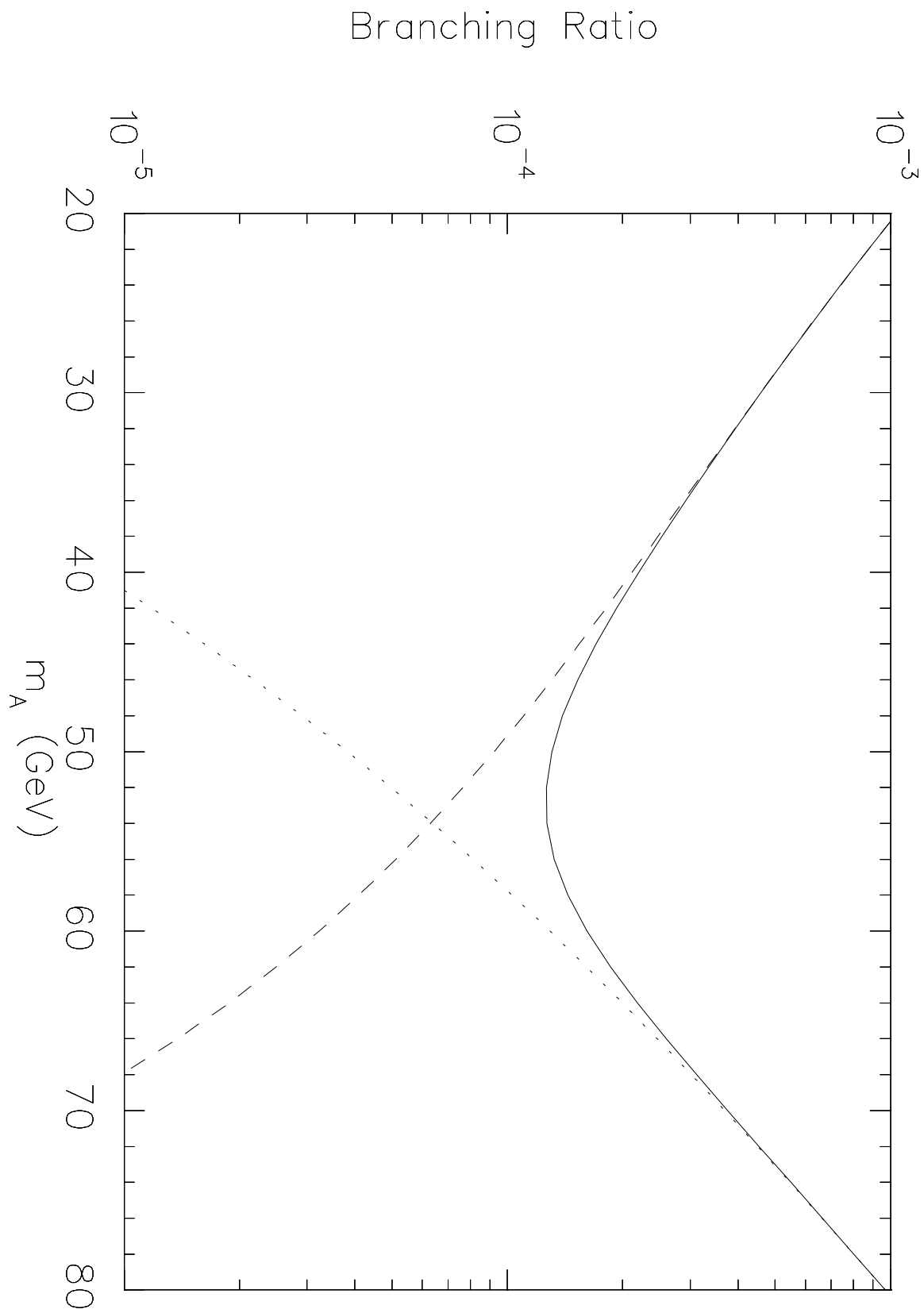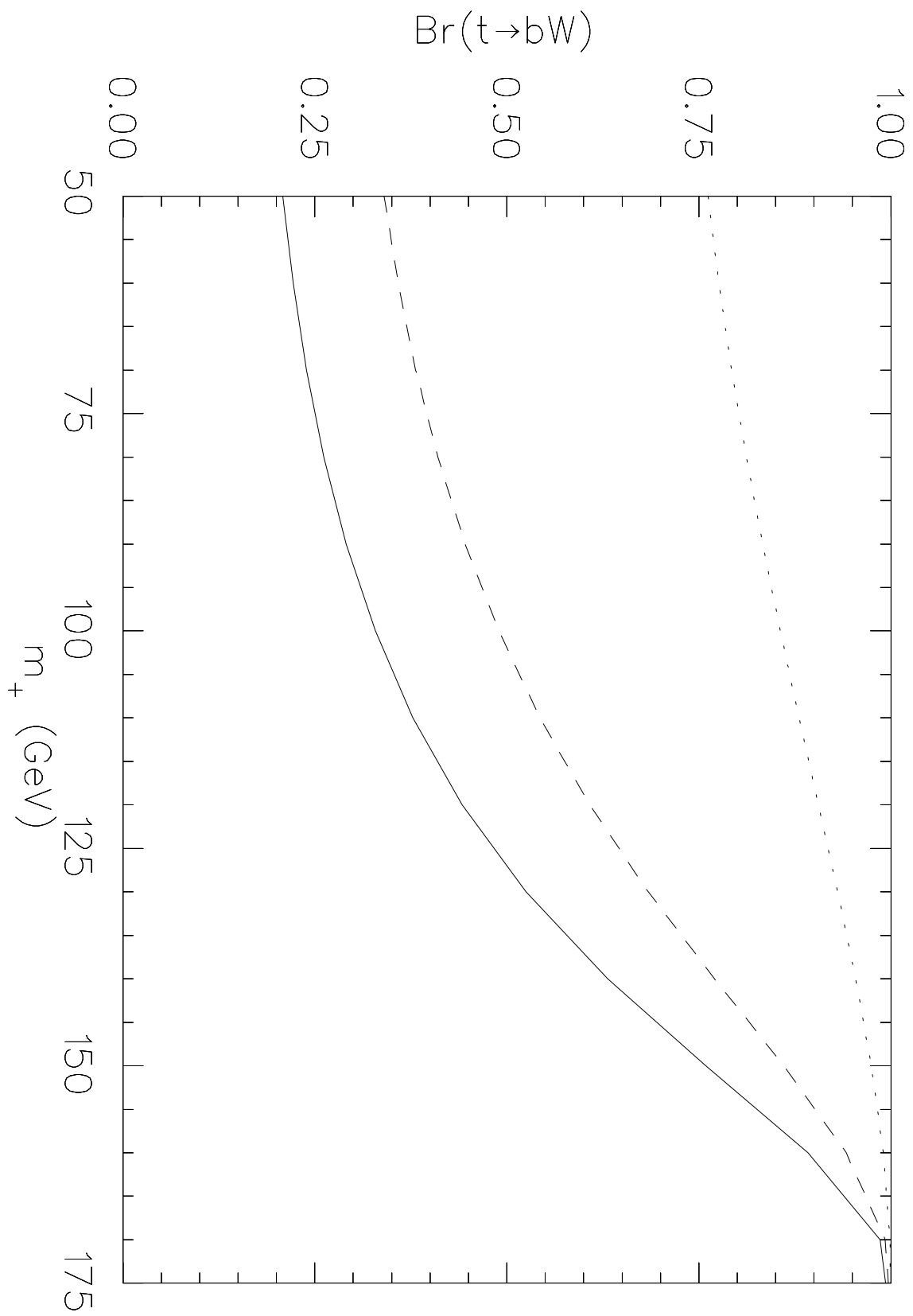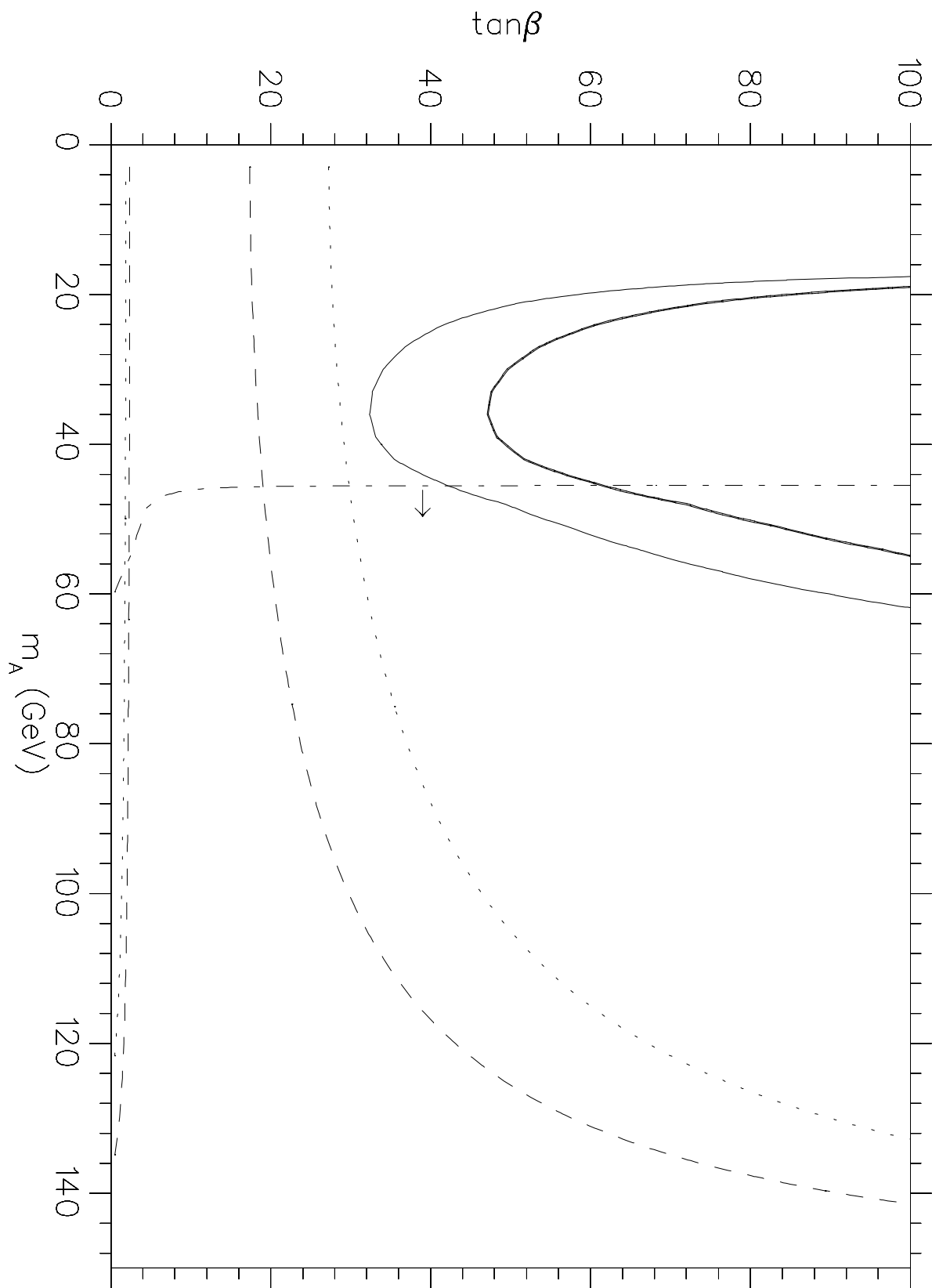
Figure 1

Branching Ratio

Figure 2

17

Figure 3

18
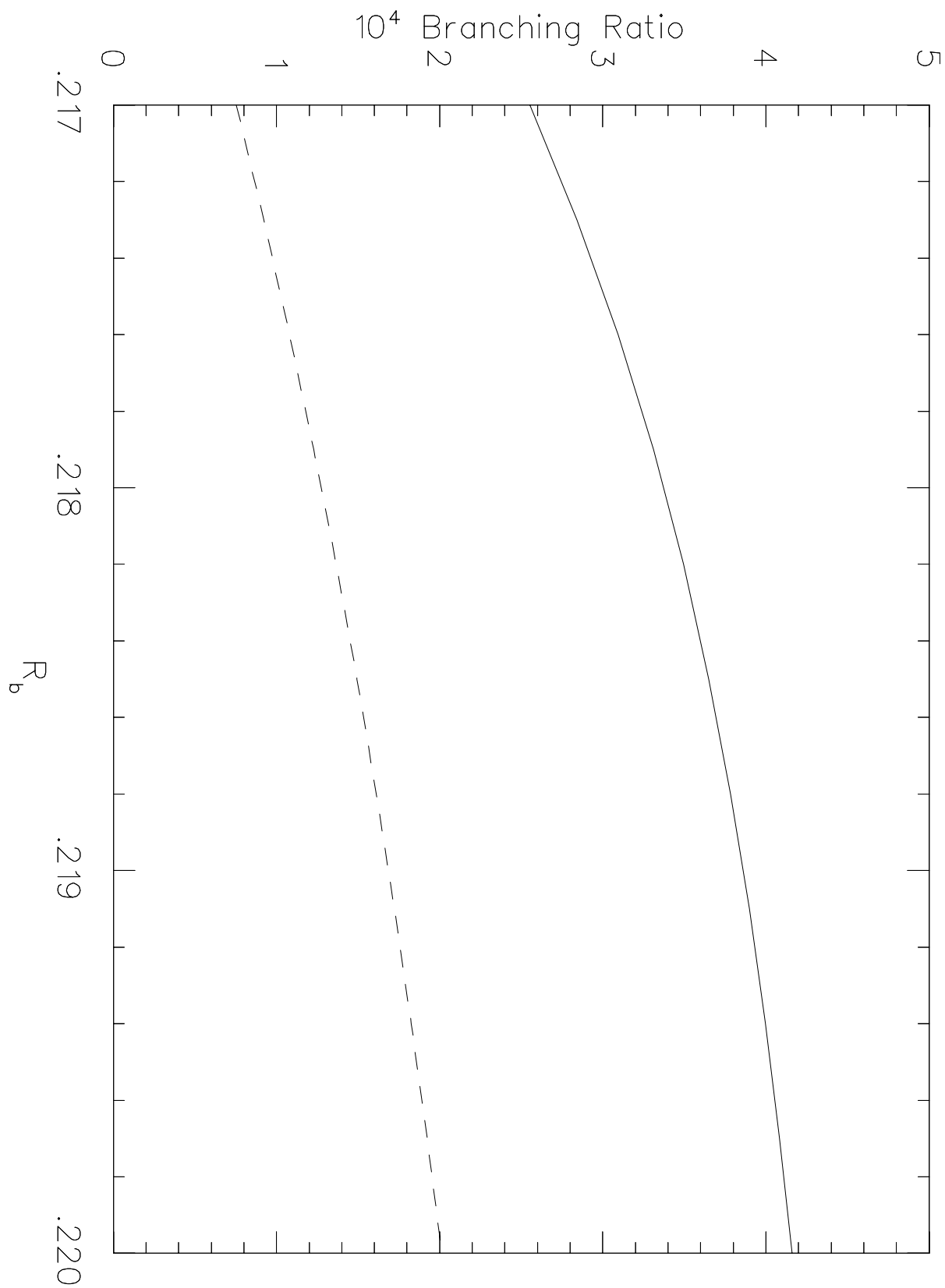
Figure 4

Figure 5

Figure 6

Figure 7

22

Figure 8